

The ^{13}C Suess effect in the world surface oceans and its implications for oceanic uptake of CO_2 : Analysis of observations at Bermuda

Robert B. Bacastow, Charles D. Keeling, Timothy J. Lueker, and Martin Wahlen

Scripps Institution of Oceanography, University of California at San Diego, La Jolla

Willem G. Mook

Isotope Physics Laboratory, University of Groningen, Netherlands

Abstract. Surface ocean water $\delta^{13}\text{C}$ measurements near Bermuda are examined in an attempt to find the annual decrease caused by the addition of anthropogenic CO_2 to the atmosphere. We refer to this trend as the surface ocean ^{13}C Suess effect. Interannual variability, which may be related to the El Niño - Southern Oscillation in the Atlantic Ocean, is apparent. We try to correct the data for this variability so as to better determine the trend. The trend has implications for the uptake of anthropogenic CO_2 by the oceans. We employ a three-dimensional model of ocean chemistry to relate the trend at Bermuda to the average ocean trend, then use the average ocean trend to estimate the vertical diffusivity K in a one-dimensional ocean model, and finally use this model to calculate the oceanic uptake of CO_2 . Uncertainties associated with the estimation of the Suess effect at Bermuda and in the analysis procedure preclude a firm estimate of the oceanic uptake of CO_2 . Results are, in general, consistent with the low side of the Intergovernmental Panel on Climate Control estimation of $2.0 \pm 0.8 \text{ GtC yr}^{-1}$. With a longer record at Bermuda and $\delta^{13}\text{C}$ observations at additional locations, we believe this approach will lead to a useful estimate of oceanic uptake.

Introduction

The ^{13}C Suess effect in the atmosphere, oceans, and land biosphere has recently been much discussed because observation of this effect has implications for the estimation of the uptake of anthropogenic CO_2 by the oceans. The ^{13}C Suess effect refers to the reduction in $\delta^{13}\text{C}$ in a reservoir due to the uptake of CO_2 produced by combustion of fossil fuel and from land clearing [Keeling, 1979]. Fossil fuel CO_2 is depleted in ^{13}C due to fractionation in its formation through photosynthesis. The oceanic uptake is open to question because the budget for CO_2 does not quite balance: when the input of fossil fuel CO_2 is added to an estimate of the input of CO_2 from land clearing and regrowth, the result is larger than the observed change in atmospheric storage and model calculated oceanic uptake. This so-called "missing CO_2 " is about $1.4 \pm 1.5 \text{ GtC yr}^{-1}$ [Houghton *et al.*, 1995]. There are at least two possible explanations: (1) the estimated oceanic uptake is too small, and/or (2) carbon is being stored in the biosphere because of fertilization due to increased atmospheric CO_2 and/or increased available nitrogen from anthropogenic sources.

An advantage in inferring the oceanic uptake of CO_2 from the Suess effect in the oceans is that the time dependence of the atmospheric input $\delta^{13}\text{C}$ signal is more similar to that of fossil

fuel CO_2 than other tracers that have been used to calibrate models, as has recently been pointed out by Heimann and Maier-Reimer [1994]. Fossil fuel CO_2 has approximately followed an exponential increase; $\delta^{13}\text{C}$ has approximately followed an exponential decrease with a similar time constant. Oceanic carbon cycle models have most often been calibrated with ^{14}C . Nuclear bomb-produced ^{14}C , however, is close to a spike centered in the mid-1960s, and natural ^{14}C has almost constant recent atmospheric input and a decay time near 8000 years.

Current Methods for Estimating Oceanic Uptake of CO_2 from ^{13}C Data

Quay *et al.* [1992] (hereafter referred to as QTW) have proposed an apparently model independent method for estimating the oceanic uptake of CO_2 . The method involves the measurement of the rate of change of the entire ^{13}C inventory in the oceans and atmosphere, and will be called the " ^{13}C inventory method". The measurement of the change in inventory in the atmosphere is straight forward because the atmosphere is relatively well mixed and measurements of its ^{13}C increase are ongoing. Determining the change in the oceanic inventory is, however, more difficult. QTW extended the significance of seven available profiles of change in $\delta^{13}\text{C}$ between 1970 and 1990 by relating the depth-integrated change in this tracer to the corresponding change in $\Delta^{14}\text{C}$, due to nuclear bombs, at nearby locations as measured during the Geochemical Ocean Sections Study (GEOSECS) program during the early 1970s. They then used the total bomb $\Delta^{14}\text{C}$ change in the ocean as measured dur-

Copyright 1996 by the American Geophysical Union.

Paper number 96GB00192.
0886-6236/96/96GB-00192\$12.00

ing the GEOSECS program to estimate an average oceanic Suess effect between 1970 and 1990, and a corresponding oceanic uptake.

Broecker and Peng [1993] have critically examined the ^{13}C inventory method. They conclude that uncertainty in the size of the exchange fluxes between the atmosphere and the land biota, and between the atmosphere and the ocean, and uncertainty in the effective size of the oceanic reservoir for $\delta^{13}\text{C}$, make the ^{13}C inventory method estimate of oceanic CO_2 uptake too uncertain to distinguish among carbon budgets currently being considered. (The effective size of the ocean reservoir involves both the ratio of the Suess effect in the surface ocean to that in the atmosphere and the penetration depth of $\delta^{13}\text{C}$ into the oceans).

Tans *et al.* [1993] (hereafter referred to as TBK) also examined the QTW ^{13}C inventory approach. They point out the uncertainty introduced by (1) the ^{13}C disequilibrium between the atmosphere and the land biota associated with Suess effect in the land biota (which is probably impossible to measure directly because of the diversity of the biota and so must be modeled), (2) possible calibration offsets between 1970 and 1990 (the measurements were done by different people using different instrumentation), and (3) ^{13}C transports within the ocean that have no ^{14}C analog (for example, transport associated with the change in fractionation in ocean photosynthesis due to change in dissolved CO_2 concentration [Rau *et al.*, 1989; Jasper and Hays, 1990]).

TBK have suggested a second approach: the "air-sea ^{13}C disequilibrium method", which, they have shown, gives quite a different estimate for oceanic uptake of CO_2 . The ^{13}C inventory method of QTW is based on a ^{12}C and ^{13}C balance on the atmosphere and ocean taken together; the air-sea ^{13}C disequilibrium method is based on a similar balance but only for the atmosphere. TBK point out that the air-sea disequilibrium method has the advantage that measurements can all be made at one time, but appropriate measurements would need to be very extensive.

The most important term in TBK's equation for oceanic CO_2 uptake is the air-sea ^{13}C disequilibrium term:

$$F_{ma}(\delta_a^e - \delta_a) \quad (1)$$

where

$$\delta_a^e = \alpha_{ma}/\alpha_{am} + \delta_m - 1 \quad (2)$$

Here F_{ma} denotes the gross flux from the ocean to the atmosphere, (α_{ma}/α_{am}) the temperature dependent equilibrium fractionation factor for the atmosphere relative to the surface ocean, δ_a the $\delta^{13}\text{C}$ of atmospheric CO_2 , and δ_m the $\delta^{13}\text{C}$ of dissolved inorganic carbon in the surface oceans. (The above equations are approximations that are valid because the α 's are near 1 and the δ 's are small compared to unity.) One must specify δ_a , δ_m , and temperature everywhere over the surface oceans. Both δ_a and δ_m vary seasonally and interannually, as will be shown below for δ_m . The uncertainty associated with the land biota ^{13}C disequilibrium also contributes to the uncertainty in the estimate of ocean uptake by this method.

Heimann and Maier-Reimer [1994] (hereafter referred to as HMR) have reviewed both of the above methods and suggest a third approach: the "dynamic constraint" method. This method is based on the assumption that the penetration depth into the

ocean of $^{13}\text{CO}_2$ and stable carbon CO_2 (i.e., the sum of $^{13}\text{CO}_2$ and $^{12}\text{CO}_2$) are essentially the same because the input time dependence of the signals has been almost the same. The method avoids the uncertainty caused by the Suess effect in the land biota, and uses the average Suess effect in the oceans between 1970 and 1990 found by QTW to estimate a more precise value for the oceanic uptake than with the ^{13}C inventory method. HMR go on to show that the three methods discussed above lead to a consistent composite oceanic uptake of $2.10 \pm 0.93 \text{ GtC yr}^{-1}$ if small adjustments to the carbon cycle parameters are made, as indicated by a "total inversion" technique.

Another Method for Estimating Oceanic Uptake from ^{13}C Data

We propose a fourth approach, based on observation of the Suess effect in the ocean surface waters. This method requires two ocean models: a three-dimensional model of the Suess effect in the world surface oceans and a one-dimensional, areally averaged, parameterized model of oceanic CO_2 uptake. Both models need to be coupled to a model of the land biota. The method also requires atmospheric CO_2 and fossil fuel input records since the beginning of the fossil fuel era. The idea is to use the three-dimensional model to infer the average surface ocean Suess effect from time series observations at particular locations, and then to use this average surface Suess effect to calibrate the one-dimensional model.

Our view is that the atmosphere is supplying CO_2 and $\delta^{13}\text{C}$ to the surface ocean, and this signal is drained away by mixing with deeper water in a similar way for both $\delta^{13}\text{C}$ and CO_2 . Thus $\delta^{13}\text{C}$ serves in place of dissolved inorganic carbon concentration (DIC) as the tracer of CO_2 uptake. The problem with using DIC itself is that the effective atmospheric exchange time of about 8 years for $^{13}\text{CO}_2$ is reduced to less than 1 year for CO_2 by the chemical buffering of CO_2 by dissolved bicarbonate and carbonate ions in seawater [Revelle and Suess, 1957], so that the variation in DIC in surface water is constrained to closely track the variation in atmospheric $p\text{CO}_2$, and is consequently insensitive to uptake of CO_2 by deeper water. Since transport to deeper water is similar for both $\delta^{13}\text{C}$ and CO_2 , if the one-dimensional model is adjusted to predict the observed surface ocean Suess effect, it should also predict the uptake of CO_2 , with good reliability.

For the three-dimensional model, we adopt a carbon cycle model based on the circulation field from an oceanic general circulation model (OGCM). With this model, we predict, to a first approximation, the Suess effect in the global surface ocean.

For the one-dimensional model, we use the box diffusion model [Oeschger *et al.*, 1975], in which transport is parameterized by an eddy diffusivity, K , which specifies the transfer of both isotopes of CO_2 from the surface water to deeper water. We will examine how CO_2 uptake and the surface water Suess effect vary with K , and find the value of K and range of uncertainty consistent with the observed $\delta^{13}\text{C}$ time series data.

The box diffusion model employed here does not include the ocean carbonate cycle, riverine inputs, or the effect of the ocean biota. These effects are shown by TBK and HMR to have relatively small influence on the estimate of CO_2 uptake by the three methods previously discussed, and they can be included at a later time, if found to contribute measurably to the result.

We first discuss the determination of the Suess effect from $\delta^{13}\text{C}$ data in surface water near Bermuda. This discussion is somewhat lengthy because of the need to separate out the seasonal cycle and the interannual variation. Having an estimate of the long-term trend in the waters near Bermuda, we then present three-dimensional model predictions of the Suess effect in the world ocean surface waters, then estimate the average surface ocean ^{13}C Suess effect, and finally discuss implications for the oceanic uptake of fossil fuel CO_2 based on the box diffusion model. Our objective is more to examine the methodology than to come to a definitive conclusion about oceanic uptake. In such a study, it is useful to confront real data. At present, Bermuda is the only location where suitable data are available, but useful data from a station near Hawaii arc anticipated in a few years.

Bermuda $\delta^{13}\text{C}$ Surface Water Observations

Flask samples of seawater were collected approximately monthly at Station S (at 32°N , $64\frac{1}{2}^\circ\text{W}$) near Bermuda Island, and analyzed at Groningen, The Netherlands, through August, 1990, and at Scripps Institution of Oceanography (SIO) thereafter (except for the October, 1990, sample, which was analyzed at Groningen) (T. J. Lueker et al., Inorganic carbon variations in surface ocean water near Bermuda, to be submitted to the *Journal of Marine Chemistry*, 1996). Two flasks were collected at each of two depths, approximately 2 m and 10 m. Flask measurements at each depth were averaged, and then the results at each depth were averaged together to make a daily average. The daily averages were employed in subsequent analysis. The program is ongoing; we will consider the first 10 years of the record, beginning with September, 1983, and extending into 1993.

Replicate flasks were used to estimate a standard error of 0.019‰ for the mean of the analyses of a pair of flasks at a single depth (T. J. Lueker et al., 1996). Data for duplicate flask samples at a particular depth were normally discarded if the difference between them exceeded 0.057‰ (3 standard deviations of the mean). However, if only one measurement disagreed with the three others collected during the same day (including the pair at the other depth sampled), by more than 0.057‰ , then only the single measurement was discarded. For the 10-year record, 7 pairs and 14 single measurements were discarded out of 207 measurements.

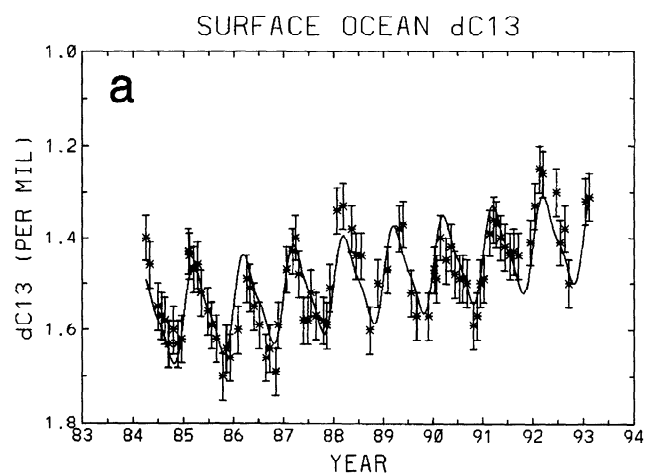


Figure 1a. Daily averages of $\delta^{13}\text{C}$ (‰) at Bermuda Station S, fit by a straight line to represent interannual change, plus harmonics of 12- and 6-month period to represent the seasonal cycle.

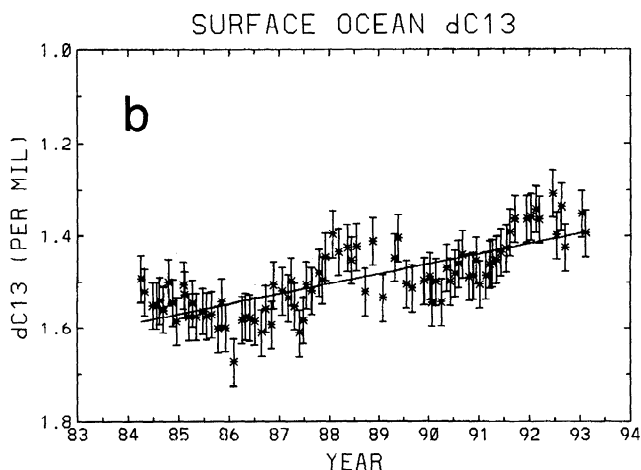


Figure 1b. Daily averages of $\delta^{13}\text{C}$ at Bermuda Station S, seasonally adjusted by the 12- and 6-month period harmonics from the fit described above for Figure 1a. The curve is the straight line part of the fit. The slope of the line (^{13}C Suess effect per year) is $-0.022 \pm 0.002 \text{‰ yr}^{-1}$.

tions of the mean). However, if only one measurement disagreed with the three others collected during the same day (including the pair at the other depth sampled), by more than 0.057‰ , then only the single measurement was discarded. For the 10-year record, 7 pairs and 14 single measurements were discarded out of 207 measurements.

To measure a small change per year in $\delta^{13}\text{C}$ (the Suess effect in the surface ocean is only about -0.02‰ yr^{-1} , see below), one must be concerned about discontinuities in procedure and in long-term drift of the mass spectrometer used in the measurements. The change between analysis at Groningen and at SIO was examined by analyzing, at both Groningen and SIO, samples of three sodium carbonate solution standards with $\delta^{13}\text{C}$ near to that of air. The difference, SIO - Groningen, was $-0.007 \pm 0.022 \text{‰}$. No correction has been made for this very small difference. Drift studies and N_2O corrections for earlier data analyzed at Groningen are discussed by Mook et al. [1983]. Similar studies are underway at SIO.

To find the Suess effect in the Bermuda data, the daily averages of $\delta^{13}\text{C}$ were fit simultaneously with a straight line in time, to represent interannual change, and harmonics with periods of 12 and 6 months, to represent the seasonal cycle. The data and fitted curve are shown in Figure 1a. Note that the ordinate (y axis) is plotted decreasing upward. This is done to correspond to our convention for atmospheric $\delta^{13}\text{C}$, chosen so that an increase in CO_2 from either fossil fuel combustion, biota respiration, or land clearing will produce an upward change in $\delta^{13}\text{C}$. Thus the CO_2 and $\delta^{13}\text{C}$ changes will be in the same direction in the atmosphere when due to the above phenomena.

The straight line part of the fit has a slope, the average annual ^{13}C Suess effect, of $-0.022 \pm 0.002 \text{‰ yr}^{-1}$. However, interannual variability with a period of 3 to 5 years is apparent in the seasonally adjusted data, Figure 1b. This variability causes uncertainty in the determination of the average annual Suess effect. The seasonally adjusted data points are not statistically independent, as implicitly assumed in the fitting pro-

cedure, so the error on the slope above is not valid. Indeed, this interannual variability, if present generally, considerably complicates the air-sea ^{13}C disequilibrium analysis of TBK.

The magnitude of the error plotted for each point is calculated from the reduced chisquared of the fit, as is also the error on the slope given above. These errors thus include natural variability as well as sampling and analysis error. They are much larger than the sampling and analysis error alone, which is ordinarily only about 0.014‰ for each daily average, since flask averages at two depths were combined to form the daily average. The analysis and sampling error bars would extend only a little further than the plotting symbol.

Extracting the ^{13}C Suess effect from surface water observations is reminiscent of the problem of determining the airborne fraction from atmospheric measurements at Mauna Loa, Hawaii, or the south pole. At these locations, atmospheric CO_2 shows variability on a 3- to 5-year timescale that correlates with the El Niño - Southern Oscillation phenomena (ENSO) [Bacastow, 1976; Keeling *et al.*, 1989]. We have not found a good way to remove the effect of this variability in atmospheric CO_2 concentration; the irregular timing of the 3- to 5-year CO_2 variability correlates well with the ENSO indices with which we are familiar (based on atmospheric pressure differences across the Pacific Ocean or sea surface temperatures in the central equatorial Pacific Ocean) [Keeling *et al.*, 1989], but the magnitude of the variations do not correlate well with the magnitude of the indices. Our solution for atmospheric data has been to measure the airborne fraction between corresponding phases of the ENSO. The uncertainty due to this variability declines as the time series becomes longer.

With the Bermuda $\delta^{13}\text{C}$ data, however, T. J. Lueker *et al.* (1996) have shown that if they confine their analysis to the values of $\delta^{13}\text{C}$ occurring at the minimum measured temperature during the winter of each year, and regress these $\delta^{13}\text{C}$ values against the minimum temperatures, the fit can be much improved by adjusting each measurement by an estimate of the Suess effect. The error in the Suess effect per year found by this method is determined from the width of the associated likelihood function. The result is -0.018 ± 0.005 ‰ yr^{-1} . In

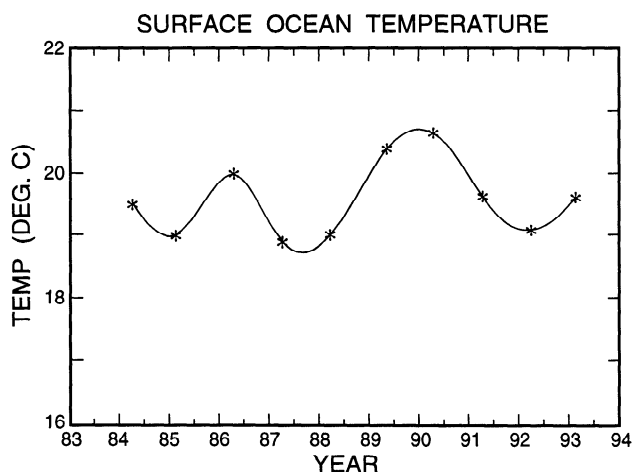


Figure 2. Yearly minimum temperatures at Station S ($^{\circ}\text{C}$), fit by a Reinsch-type spline with a very small error per point (0.02°C).

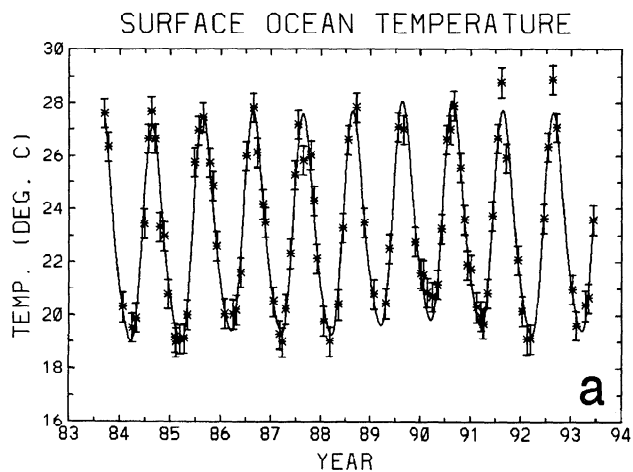


Figure 3a. All temperature measurements at Station S associated with $\delta^{13}\text{C}$ measurements ($^{\circ}\text{C}$), fit by a Reinsch-type spline plus harmonics with 12- and 6-month periods. The error per point to produce this fit is 0.55°C .

trying to understand why this procedure seems to work so well, and attempting to improve it, we repeat this analysis in a way that can be extended to the data for all seasons.

We first fit a Reinsch-type spline [Reinsch, 1967] with very small assigned error per point (0.02°C) to the annual minimum temperatures versus time. This spline (Figure 2) reveals a variation with ENSO-like periodicity. We then fit all of the temperature measurements in surface water at Station S, associated with measurements of $\delta^{13}\text{C}$, simultaneously by a Reinsch-type spline and a seasonal cycle represented by 12- and 6-month harmonics (Figure 3a). The procedure for the fit was approximately the same as has been used for atmospheric CO_2 data [Keeling *et al.*, 1989]. In fitting a Reinsch-type spline, one may vary a parameter that is equivalent to reduced chisquared, or alternately, set the reduced chisquared parameter equal to the number of degrees of freedom for the fit, and vary the value of the error

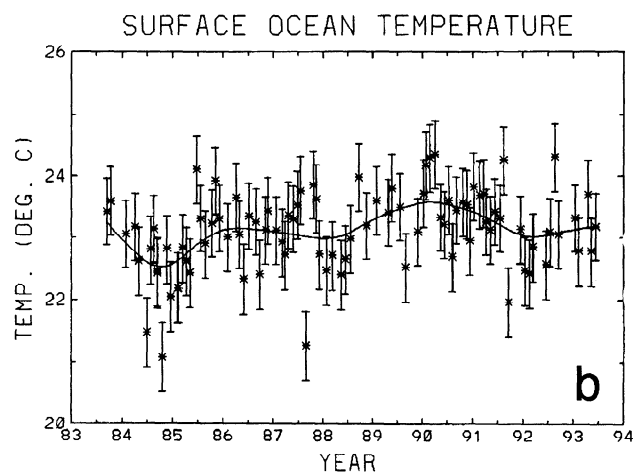


Figure 3b. All temperature measurements at Station S associated with $\delta^{13}\text{C}$ measurements ($^{\circ}\text{C}$), seasonally adjusted by the 12- and 6-month period harmonics from the fit described above for Figure 3a. The curve is the spline part of the fit.

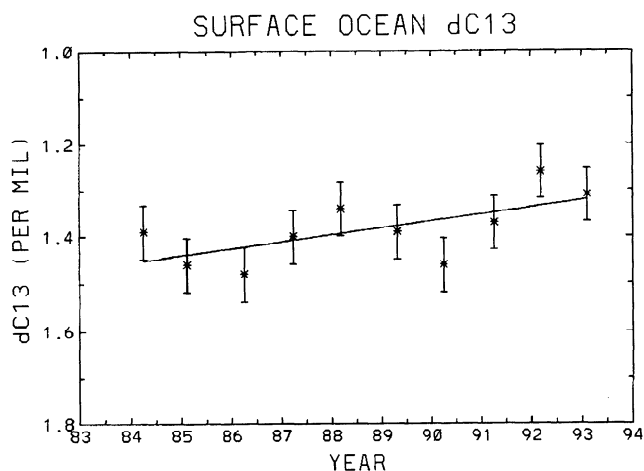


Figure 4. Daily averages of $\delta^{13}\text{C}$ (‰) associated with the minimum temperature measurement during the year, fit by a straight line. The slope of the line is -0.015 ± 0.11 ‰ yr^{-1} .

per point, with all points assumed to have the same error. The latter procedure was chosen, and the error per point varied to obtain a spline with a stiffness that reasonably captures the non-seasonal variability. The number of degrees of freedom associated with the spline was arbitrarily set to 3. The fit was obtained by iteratively fitting the spline to the residuals of the seasonal cycle fit, and then the seasonal cycle to the residuals of the spline fit. Ten iterations were sufficient to produce an essentially invariant fit. The spline found in this way, shown in Figure 3b, represents the interannual variability in the temperature. It is very similar in shape to the spline fit to minimum temperatures shown in Figure 2, except that the strong minimum in late 1987 is somewhat suppressed.

Next, the winter time analysis of T. J. Lueker et al. (1996) was repeated by fitting the $\delta^{13}\text{C}$ daily averages at minimum measured yearly temperature with a straight line in time (Figure 4). The slope of this line, 0.015 ± 0.110 ‰ yr^{-1} , is not significantly different from zero owing to the scatter caused by the interannual variability. Then the $\delta^{13}\text{C}$ values were fit to a straight line in time plus the temperature spline of Figure 2:

$$\delta^{13}\text{C}_{\text{fit}} = a + bt + cT_{\text{sp}}(t) \quad (3)$$

where t is time (years), $T_{\text{sp}}(t)$ ($^{\circ}\text{C}$) is the time dependent temperature spline of Figure 2, and a , b , and c are constants determined by the fitting procedure. The resulting fit (Figure 5a), in which the constant coefficient of the temperature spline, c , is negative, closely follows the observations. The slope of the straight line part of the fit, b , in agreement with the analysis of T. J. Lueker (1996) mentioned above, is -0.018 ± 0.005 ‰ yr^{-1} , significantly different from zero (Figure 5b).

All of the daily averaged $\delta^{13}\text{C}$ values were then fit with a straight line in time plus T_{sp} , the spline of Figure 2, plus harmonics with 12- and 6-month periods (Figure 6a). The temperature spline follows quite well the interannual variability of the surface ocean $\delta^{13}\text{C}$ measurements (Figure 6b). The slope of the straight line (Figure 6c) is -0.025 ± 0.002 ‰ yr^{-1} . The error associated with this estimate, 0.002 ‰ yr^{-1} , is considerably less

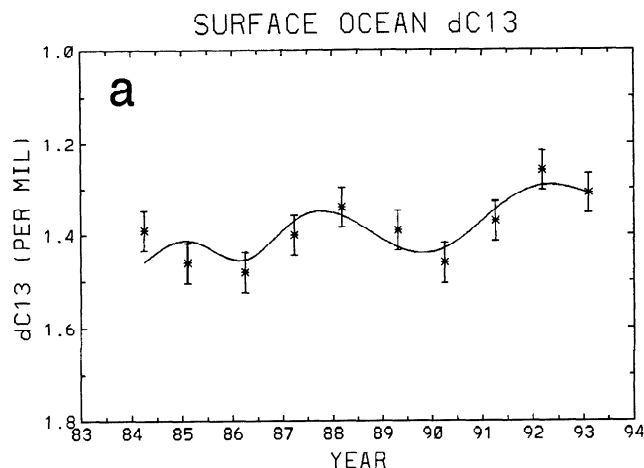


Figure 5a. Daily averages of $\delta^{13}\text{C}$ (‰) associated with the minimum temperature measurement during the year, fit by a constant times the spline of Figure 2 plus a straight line.

than the error associated with the fit to only the $\delta^{13}\text{C}$ values at annual minimum temperature, 0.005 ‰ yr^{-1} .

In trying to understand the role of temperature in these winter minimum and all seasonal fits, we hypothesize that year-to-year variation in minimum-observed temperature represents variation in the amount of deep water which is mixed into the surface water, or the depth from which it comes. Deeper water is tagged with lower temperature, more depleted ^{13}C , and higher nutrient concentrations. The nutrients mixed into surface water from deeper water fuel photosynthesis, which tends to cancel out that part of the $\delta^{13}\text{C}$ depletion associated with the nutrients, leaving a deeper water Suess effect signal proportional to the upwelling amount and thus to the yearly minimum temperature variation.

Analysis of dissolved inorganic carbon (DIC) concentration tends to support the explanation above. The DIC measurements

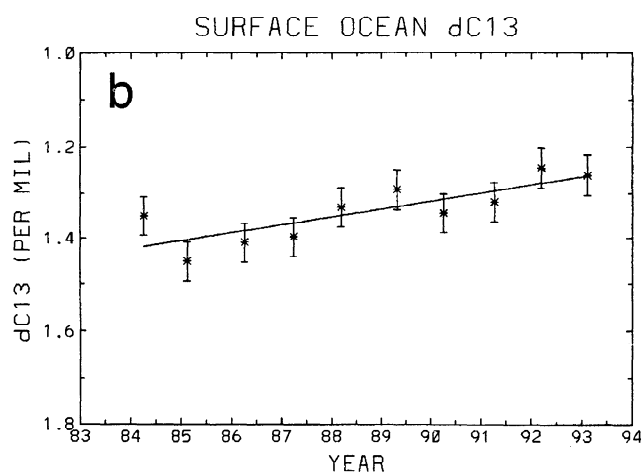


Figure 5b. Daily averages of $\delta^{13}\text{C}$ (‰) associated with the minimum temperature measurement during the year, adjusted for interannual variation by the spline part of the fit described above for Figure 5a. The curve is the straight line part of the fit. The slope of the line is -0.018 ± 0.005 ‰ yr^{-1} .

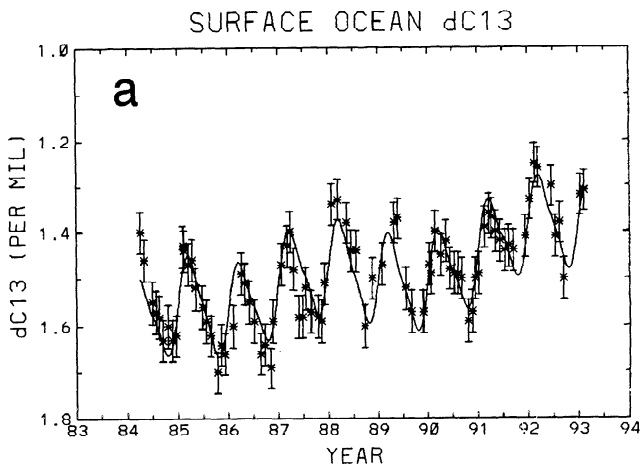


Figure 6a. Daily averages of $\delta^{13}\text{C}$ (‰), fit by a constant times the temperature spline of Figure 2 plus a straight line plus harmonics of 12- and 6-month period.

have been fit with a Reinsch-type spline and 12- and 6-month harmonics (Figure 7a). Deeper, colder water has higher DIC concentration than shallower water mainly because of remineralization of organic carbon detritus. The nonseasonal, spline part of the fit of DIC (Figure 7b) shows structure which resembles the nonseasonal, spline part of the fit of $\delta^{13}\text{C}$ (Figure 6b). Since the vertical axis of the $\delta^{13}\text{C}$ plot is reversed, and since the $\delta^{13}\text{C}$ temperature effect is opposite to that for DIC, the patterns should correspond if due to variation in vertical mixing. Actually, the DIC spline more resembles the inverse of the spline in the temperature fit to all of the data (upper curve in Figure 7b), in that the peak in late 1987 in DIC and in inverse temperature are both somewhat suppressed compared to $\delta^{13}\text{C}$ (Figure 6b) and minimum winter temperature (Figure 2).

One should not be surprised that there is variability in the surface water and thermocline structure of the ocean near Bermuda. There is an ENSO signal in the Atlantic Ocean, delayed

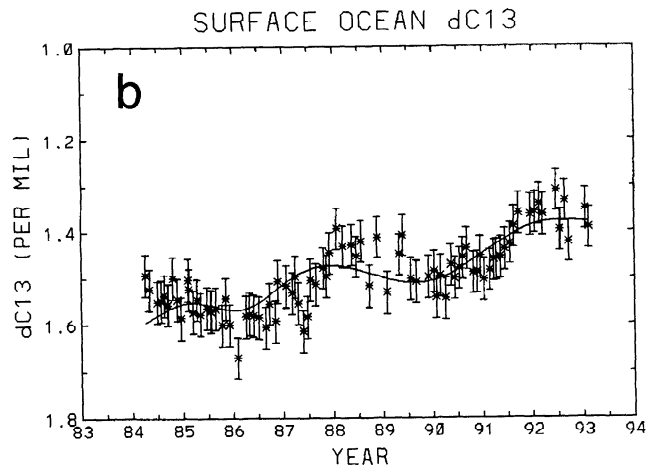


Figure 6b. Daily averages of $\delta^{13}\text{C}$ (‰), seasonally adjusted by the 12- and 6-month period harmonics from the fit described above for Figure 6a. The curve is the (fitted) constant times the temperature spline of Figure 2 plus the straight line fit above.

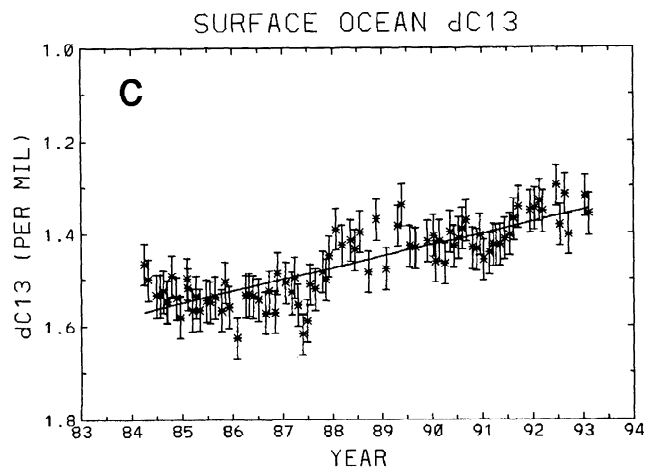


Figure 6c. Daily averages of $\delta^{13}\text{C}$ (‰), seasonally adjusted by the 12- and 6-month period harmonics described above for Figure 6a and adjusted for interannual variation by the (fitted) constant times the temperature spline of Figure 2. The curve is the straight line part of the fit. The slope of the line is -0.025 ± 0.002 ‰ yr^{-1} . For convenience in plotting, the data and curve were both adjusted so as to agree with Figure 6b at the year 1988.

from the Pacific ENSO by about 18 months [Tourre and White, 1995]. Since the equatorial warm surface water phase of the ENSO corresponds to a reduction in or cessation of equatorial upwelling, the midlatitude downwelling that supplies this upwelling must also vary.

Tourre and White [1995] find an ENSO Index for the Atlantic Ocean through a rotated empirical orthogonal function analysis of a 13-year sea surface temperature record. Their ENSO Index represents equatorial warm events, but at the latitude of Bermuda, they find that sea surface temperature anomalies tend to have the opposite phase [Tourre and White, 1995, their Figure 13]. If their index is inverted and delayed by 6 months (the higher latitude events then precede the equatorial events), as shown in Figure 8, there are peaks which line up with the warm events at Bermuda in 1986 and 1988-1989, as indicated by the fit to the winter minimum temperatures.

The mixed-layer depth at Station S deepens in the winter and early spring due to surface cooling and wind mixing, reaching a maximum depth usually in February, according to hydrographic data collected biweekly since 1954 [Menzel and Ryther, 1960]. The seasonal variation in the mixed-layer depth is large [Siegel et al., 1995]. A late summer mixed-layer depth in the neighborhood of 20 m is followed by a winter mixed-layer depth that may be greater than 200 m.

Estimates of new production, a measure of nutrients brought into the surface water, usually from below, do not correlate well with mixed-layer depth [Michaels et al., 1994]. The maximum mixed-layer depth during 1989 was 230 m, but new production was estimated to be less than in 1990, when the maximum mixed-layer depth did not exceed 160 m. However, sediment trap data suggests that the period of high production was longer in 1990 (February through May) than the corresponding period during 1989 (only February), thus probably compensating for

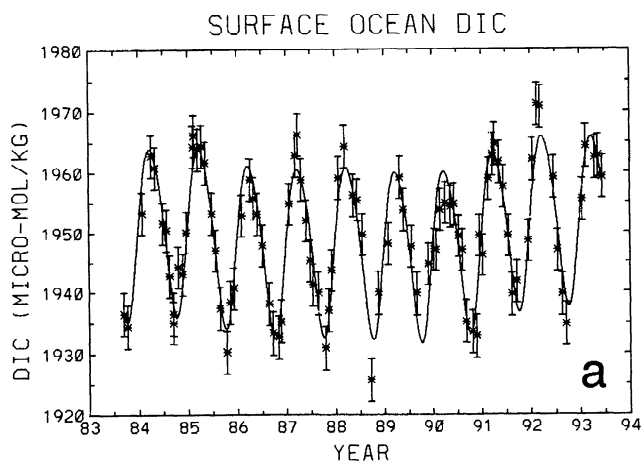


Figure 7a. Daily averages of dissolved inorganic carbon ($\mu\text{mol kg}^{-1}$), fit by a Reinsch-type spline plus harmonics with 12- and 6-month periods. The error per point to produce this fit is $3.5 \mu\text{mol kg}^{-1}$.

the shallower mixing. The annual minimum temperatures plotted in Figure 2 also do not correlate well with the annual maximum mixed-layer depths. Nevertheless, variability in minimum temperature may better indicate total mixing from deeper water than maximum mixed-layer depth because minimum temperature should tend to represent the integral of the mixing process.

In summary, we find interannual variability in the time series of $\delta^{13}\text{C}$ observations at Bermuda which tends to obscure the average annual ^{13}C Suess effect. We employ an empirical method to remove this variability, but we do not have complete understanding of the cause of the variability or why the empirical method works as well as it does.

Predicted Surface Water ^{13}C Suess Effect

Our next task is to find the relation between the surface ocean Suess effect at Bermuda and the average surface ocean

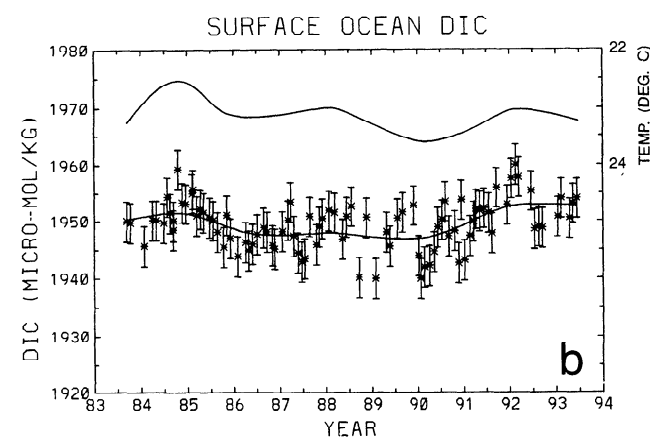


Figure 7b. Daily averages of dissolved inorganic carbon ($\mu\text{mol kg}^{-1}$), seasonally adjusted by the 12- and 6-month period harmonics from the fit described above for Figure 7a. The curve through the daily averages is the spline part of the fit. The upper curve is the inverted spline from Figure 3b, representing seasonally adjusted temperature variation. The temperature scale is indicated on the right side ordinate.

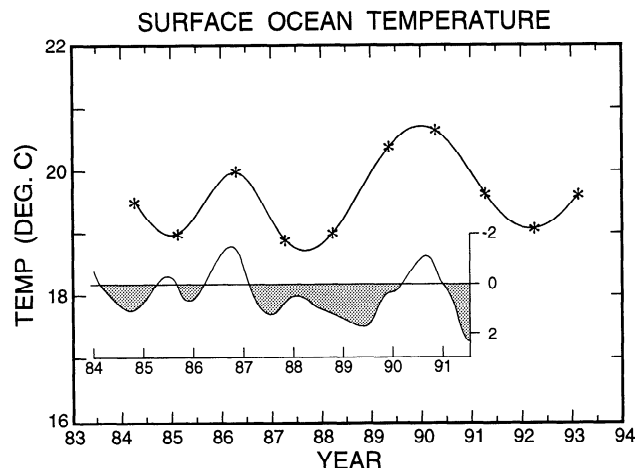


Figure 8. ENSO Index for the Atlantic Ocean, found by *Tourre and White* [1995] through a rotated empirical orthogonal function analysis of the sea surface temperature field, inverted and given a delay of 6 months, drawn below the curve of Figure 2 so as to show the similarity. The units of the ENSO Index are standard deviations.

Suess effect. We employ a three-dimensional carbon cycle model which makes use of a seasonal average of the circulation field from a 15-level ocean general circulation model (OGCM) from the Max-Planck-Institut für Meteorologie, Hamburg, Germany. Distributions of chemical species important to the carbon cycle are similar to those presented by *Maier-Reimer* [1993], who employed the seasonally varying circulation field from the same OGCM. Our biota model [*Bacastow and Maier-Reimer*, 1990, 1991], however, is somewhat simpler than *Maier-Reimer's* [1993]. Also, in our model, the atmosphere is represented by a single, well-mixed box, and the top two levels of the ocean (50 m each) are combined to form a surface mixed-layer 100 m deep, a little deeper than the annual average depth, to represent the effect of winter mixing in a seasonally averaged model. Convective mixing is parameterized by diffusion, following a method used by *Maier-Reimer and Hasselmann* [1987, and personal communication, *Maier-Reimer*, 1986]. Sea surface temperatures are assumed to have no interannual variation, so are constant at the annual average of values employed in the OGCM.

In both the three-dimensional model and the box diffusion model, the transport of stable carbon ($^{12}\text{C} + ^{13}\text{C}$) and ^{13}C are considered separately, and approximations are made that are appropriate to this system [*Keeling et al.*, 1989]. Fractionation coefficients of ^{13}C relative to stable carbon, rather than ^{12}C , differ by a small correction, and are labeled below with a "prime" ('). Final results are converted to $\delta^{13}\text{C}$, the departure from unity in the ratio of ^{13}C to ^{12}C relative to this ratio in Pee Dee belemnite (PDB) standard. The ^{13}C fractionation coefficient between atmosphere and surface mixed layer of the ocean, α_{am}' , was assigned the value 0.9982198 [*Keeling et al.*, 1989, Table 8], and the fractionation coefficient between the ocean and atmosphere was calculated from an equilibrium relation due to *Mook* [1974]:

$$\alpha_{ma}' = \alpha_{am}'(1.02389 - 9.483/T_K) \quad (4)$$

where T_K denotes the surface ocean temperature in degrees Kel-

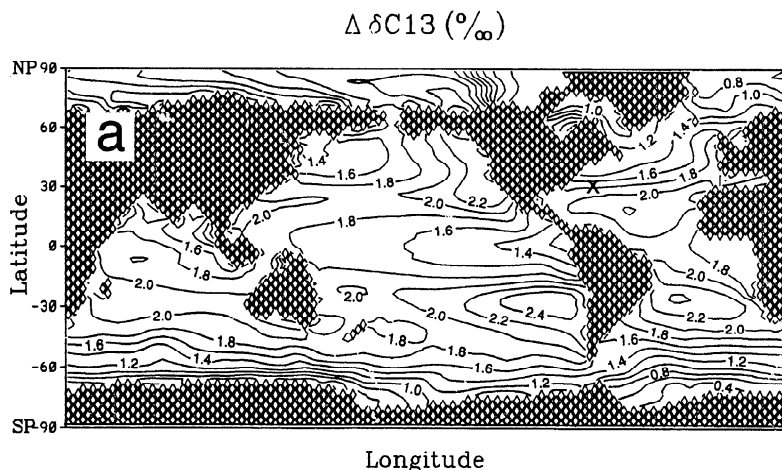


Figure 9a. Predicted surface ocean Suess effect per year (‰ yr^{-1}), depth range 0 to 100 m, for time period 1983 to 1995, multiplied by -100. The model DIC was adjusted so that the preindustrial atmospheric CO_2 concentration was near 280 ppm. The location of Bermuda is indicated by an "X".

vin. The fractionation coefficient between the ocean surface water and photosynthesized organic material, α_{mb} , is related to the difference between $\delta^{13}\text{C}$ for the organic material, $\delta^{13}\text{C}_{org}$, and $\delta^{13}\text{C}$ for the dissolved inorganic carbon in the surface mixed layer, $\delta^{13}\text{C}_m$:

$$\alpha_{mb} = 1 + \delta^{13}\text{C}_{org} - \delta^{13}\text{C}_m \quad (5)$$

For the $\delta^{13}\text{C}_{org}$, we use a relation found by Rau *et al.* [1989]:

$$\delta^{13}\text{C}_{org} = -0.8[\text{CO}_2] - 12.6 \text{‰} \quad (6)$$

where $[\text{CO}_2]$ denotes the concentration in micromoles per kilogram of dissolved CO_2 (including hydrated CO_2). Because of the uncertainty in the Rau relation above, we set $\alpha_{mb}' = \alpha_{mb}$, neglecting a small correction.

The land biota is modeled as one mixed-box initially containing 1477.44 GtC with a turnover time of 60 years [Keeling *et al.*, 1989, p. 186]. This is meant to represent long-term storage of carbon in trees and humus; short-term storage, with a turn-

over time of a year or two, would have little effect and is not included. The fractionation coefficient for land photosynthesis, α_{ab}' , was assigned the constant value 0.9820696, and α_{ba}' , the fractionation coefficient for respiration, was assigned the value 1.0 [see Keeling *et al.*, 1989, Table 8]. A fertilization flux to the land biota, proportional to the atmospheric perturbation in CO_2 , was included.

Two versions of the three-dimensional model, one with an ocean biota and one without ocean biota, were "spun-up" for 2400 model years. The average ocean alkalinity was set to approximately $2377 \mu\text{eq kg}^{-1}$. The average ocean DIC was adjusted so that the final atmospheric CO_2 concentration was close to 280 ppm. The average ocean DIC required for the models, with and without ocean biota, were $2248 \mu\text{mol kg}^{-1}$ and $2090 \mu\text{mol kg}^{-1}$, respectively. The models were run forward in time in the deconvolution mode [Keeling *et al.*, 1989, p. 195]. In this mode, the atmospheric CO_2 concentration increase is constrained to follow the observed increase, found by

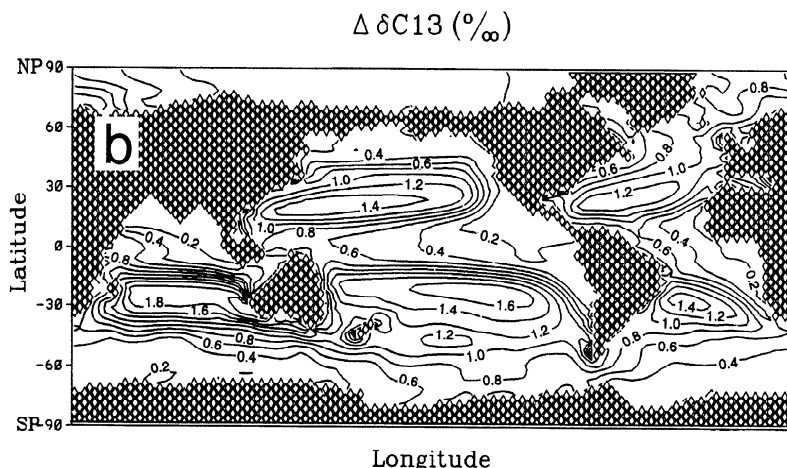


Figure 9b. Predicted Suess effect per year (‰ yr^{-1}), depth range 250 to 300 m, for time period 1983 to 1995, multiplied by -100.

differentiating a spline curve fit to observations. The spline curve is an update of the curve shown in Figure 40 of Keeling *et al.* [1989], and its construction is discussed there. Included at each time step, so as to keep the model in balance, was an additional CO_2 flux between the atmosphere and the land biota, attributable to the effect on the land biota of land clearing and regrowth, and of climatic variation.

In the deconvolution mode, the fertilization flux mentioned above has only a very small effect on atmospheric or oceanic $\delta^{13}\text{C}$. With the atmospheric CO_2 concentration and fossil fuel CO_2 input specified, and oceanic exchange calculated by the model, the net flux of CO_2 to or from the land biota is fixed independently of the fertilization flux. Since the biota has nearly the ^{13}C depletion that would be in dynamic equilibrium with the atmosphere, a larger fertilization flux would be compensated by a larger return from the land biota. (Note that the fertilization flux is small compared to the gross flux between the atmosphere and the land biota).

The predicted Suess effect in the surface ocean during the years of the Bermuda data (Figure 9a) shows a pattern of spatial variability about an average value of -0.0171‰ yr^{-1} that clearly is related to upwelling and downwelling. The Suess effect is reduced in magnitude in regions of strong upwelling, probably because one then sees the smaller Suess effect prevailing in deeper water (Figure 9b).

In the absence of an ocean biota, the predicted Suess effect is larger in magnitude by about 0.0013‰ yr^{-1} , but otherwise, the contour structure is very similar (Figure 10). The ratio of the predicted Suess effect in Bermuda surface water to the global average surface water effect is, with and without the ocean biota, almost exactly the same.

The predicted uptake of anthropogenic CO_2 by the three-dimensional model averages 1.4 GtC yr^{-1} between 1983 and 1995, as calculated in the deconvolution mode described above, and 1.6 GtC yr^{-1} in a straight forward run with no land biota. The difference is apparently due to a "pioneer" effect during early years [Siegenthaler *et al.*, 1978; Bacastow and Keeling, 1981] and to recent carbon storage in the land biota. Both of these effects are forced by the deconvolution mode. In the

deconvolution mode, the model land biota is a source to the atmosphere until about 1936, and in the absence of fossil fuel input, the atmospheric CO_2 concentration would be declining during the 1983-1995 period. Also, during this period, the land biota is taking up an annual average of about 1.2 GtC . Both effects cause the atmospheric CO_2 concentration to increase more slowly in the deconvolution mode than in the forward run with no land biota, and, consequently, the oceans take up less CO_2 .

We assume here that the variation of the surface ocean Suess effect about its areal average is correct even if the CO_2 uptake per year is not exactly correct. This assumption seems plausible; the modeled CO_2 uptake depends on deep water formation, which is very sensitive to the modeling of heat fluxes at high latitudes [Maier-Reimer *et al.*, 1993], and, consequently, somewhat uncertain. Regimes of upwelling and downwelling, however, are more directly related to the surface wind field, and more likely to be correct. Fortunately, this assumption can be checked by having data from several locations.

The predicted Suess effect near Station S from 1983 to 1995 is -0.0174‰ yr^{-1} , by happenstance, very close to the predicted global average surface Suess effect (-0.0171‰ yr^{-1}) during those years. One can see in Figure 9a that Bermuda is located in a region of high-spatial gradient in the north-south direction, and this adds to the uncertainty in the ratio of the average Suess effect to the Suess effect at Bermuda. In the following analysis we will assume from the above model results that this ratio is 1.0, so that the average surface ocean Suess effect per year is the same as that measured at Bermuda. This approximation, of course, would be replaced with a better one should more observations of $\delta^{13}\text{C}$ in seawater become available.

Implications for the Uptake of CO_2 by the Oceans

To investigate the consequence on the surface water Suess effect of variation of the model uptake of CO_2 by the oceans, we employ the box diffusion model in the deconvolution mode, coupled to the same model of the land biota as was employed

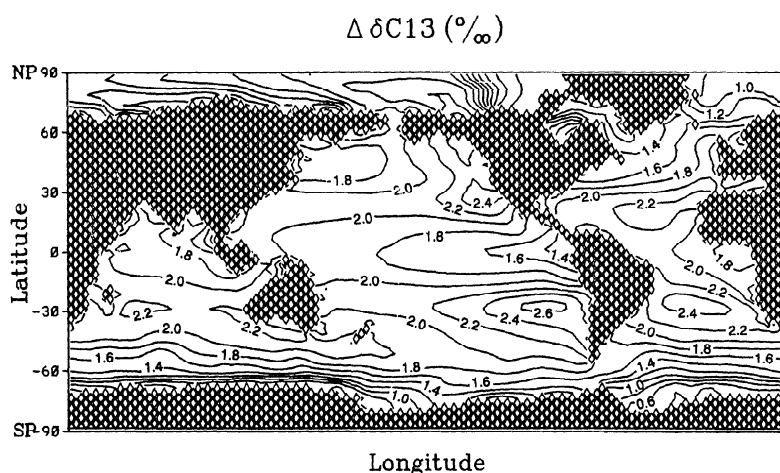


Figure 10. Predicted Suess effect per year (‰ yr^{-1}), depth range 0 to 100 m, for time period 1983 to 1995 multiplied by -100 , for model without an ocean biota. The model DIC was adjusted so that the pre-industrial atmospheric CO_2 concentration was near 280 ppm.

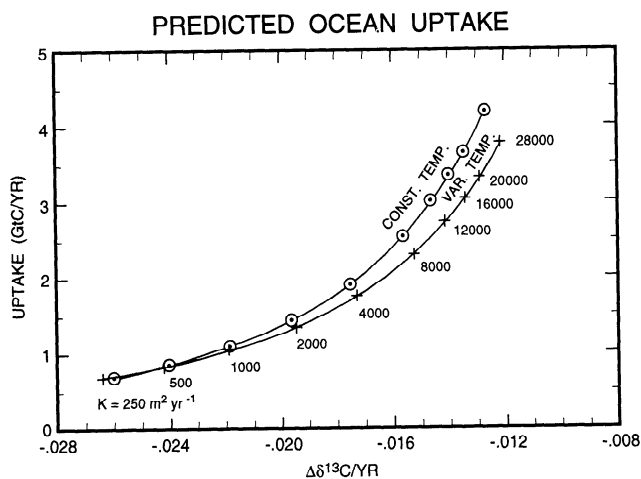


Figure 11. Predicted ocean uptake (GtC yr^{-1}) versus the change in $\delta^{13}\text{C}$ (‰ yr^{-1}) during the period 1984 to 1993 for the box diffusion model as the diffusivity K ($\text{m}^2 \text{yr}^{-1}$) is varied. The lower curve (labeled var. temp.) was obtained by varying the ocean surface temperature according to data from Jones *et al.* [1986a, 1986b, and personal communication, 1994]. The crosses and solid circles indicate the labeled values of K .

with the three-dimensional model discussed above. The diffusivity K , which controls uptake by below-surface waters, is varied to find the relationship between modeled oceanic uptake and the surface water Suess effect. The biospheric disequilibrium flux is thus included in the model in a consistent way. We examine the sensitivity of our results to the biota disequilibrium flux by varying the turnover time of the biota, τ_B , about a standard value of 60 years. The atmospheric exchange time τ_{am} was set to 6.87 years, a value appropriate for a model with K equal to $7685 \text{ m}^2 \text{yr}^{-1}$ [Siegenthaler, 1983], therefore in the middle of the expected range of K [see also Keeling *et al.*, 1989, Table 8]. The surface mixed-layer depth was set to 100 m, matching the three-dimensional model depth.

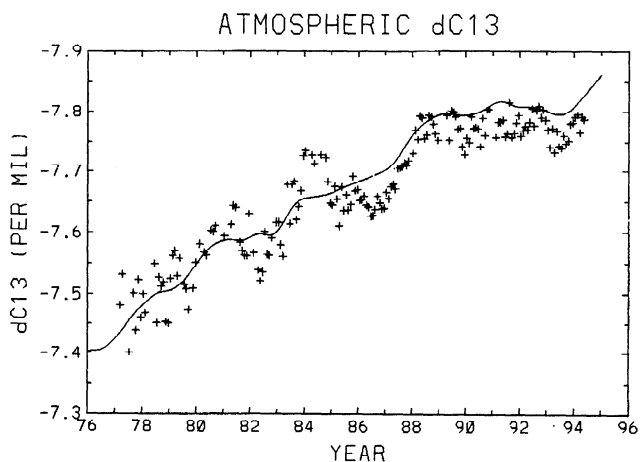


Figure 12. Atmospheric $\delta^{13}\text{C}$ measurements at Mauna Loa, Hawaii, and the south pole. The curve is a prediction from the box diffusion model describe in the text with a diffusivity K of $4000 \text{ m}^2 \text{yr}^{-1}$ and no variation of surface water temperature.

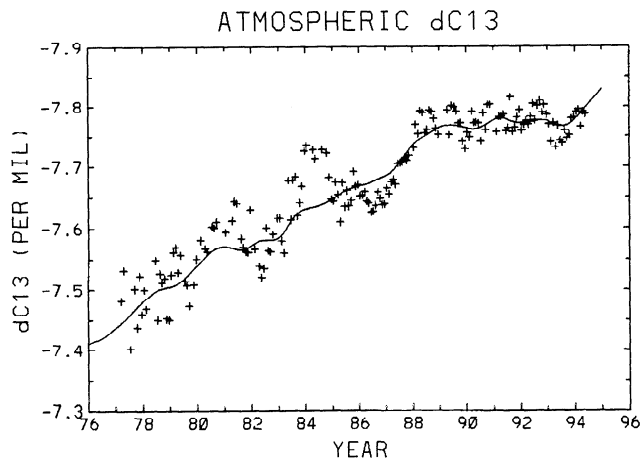


Figure 13. Atmospheric $\delta^{13}\text{C}$ measurements at Mauna Loa, Hawaii, and the south pole. The curve is a prediction from the box diffusion model describe in the text with a diffusivity K of $4000 \text{ m}^2 \text{yr}^{-1}$ and variation of surface water temperature according to data of Jones *et al.* [1986a, 1986b, and personal communication, 1994].

The resulting oceanic uptake versus $\delta^{13}\text{C}$ per year, Figure 11, is given for a global average sea surface temperature invariant with time, and one which varies with time according to data of Jones *et al.* [1986a, 1986b, and personal communication, 1994]. (These data include both land and oceanic observations, but the land-sea differences on the relatively long timescales of importance here are small.) As discussed below, the predicted decrease in atmospheric $\delta^{13}\text{C}$ from 1978 to 1995 is different depending on whether or not this temperature variation is included in the calculation. The difference in predicted oceanic uptake of CO_2 with and without variable oceanic sea surface temperature is about 0.3 GtC yr^{-1} for a modeled uptake near 2.0 GtC yr^{-1} , less for lower uptakes, and more for higher uptakes.

The model predictions appear to be more realistic if the observed variation in global average temperature is taken into account. Figure 12 shows this atmospheric $\delta^{13}\text{C}$ trend for a model with ocean surface temperature assumed constant in time and $K = 4000 \text{ m}^2 \text{yr}^{-1}$. The preindustrial atmospheric value of $\delta^{13}\text{C}$ was adjusted so that the model agrees with observations in 1978. Smaller values of K result in worse fits, larger values result in similar fits. All overpredict the observed trend. The trend is insensitive to variation of τ_B , the land biota turnover time. With time variable temperature, however, the predicted overall decrease from 1978 to near-present agrees reasonably well with observations (Figure 13).

The atmospheric trend in $\delta^{13}\text{C}$ predicted by the three-dimensional model is similar to the trend predicted by the constant temperature box diffusion model (Figure 11), but the magnitude of the change between 1978 and 1995 is larger by a very small amount (about 0.02‰). The $\delta^{13}\text{C}$ prediction before 1978 for the three-dimensional model and the constant temperature box diffusion model are close and in agreement with ice core $\delta^{13}\text{C}$ measurements, as is shown in Figure D.1 of Keeling *et al.* [1989]. (The three-dimensional model employed for Figure D.1 was a 10-level model, but predicted atmospheric $\delta^{13}\text{C}$ is essentially unchanged in the 15-level model). However, the box

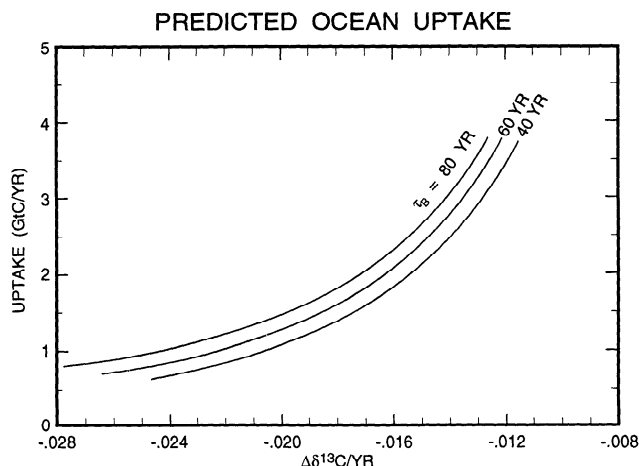


Figure 14. Predicted ocean uptake (GtC yr^{-1}) versus the change in $\delta^{13}\text{C}$ (‰ yr^{-1}) during the period 1987 to 1993 for the box diffusion model as the diffusivity K ($\text{m}^2 \text{yr}^{-1}$) is varied for biota turnover times τ_B of 40 years, 60 years, and 80 years. Temperature of the surface water was varied according to data of Jones *et al.* [1896a, 1986b, and personal communication, 1994]. The middle curve is the same as the lower curve in Figure 11.

diffusion model predictions with variable temperature are also in agreement with the more scattered ice core $\delta^{13}\text{C}$ measurements.

The box diffusion model predictions of oceanic uptake of CO_2 compared to surface ocean $\delta^{13}\text{C}$ are relatively insensitive to the land biota turnover time, τ_B , as can be seen in Figure 14. With the atmospheric CO_2 concentration constrained to follow observations, the role of the land biota is of only limited significance.

The modeling results are also relatively insensitive to variation of the atmospheric exchange time τ_{am} . An increase in τ_{am} of 1 year, with K set so that the uptake is 2 GtC yr^{-1} , decreased the oceanic uptake by only 0.1 GtC yr^{-1} , and less for smaller uptakes.

We have two estimates of the trend in surface ocean $\delta^{13}\text{C}$: (1) from the fit of all the daily averages by the temperature spline plus a straight line in time plus harmonics (Figure 6), which gives $-0.025 \pm 0.002 \text{ ‰ yr}^{-1}$, and (2) from the fit of only the yearly observations at minimum observed temperatures by the temperature spline plus a straight line in time (Figure 5), which gives $-0.018 \pm 0.005 \text{ ‰ yr}^{-1}$. Because of the large error on the latter result, the indicated CO_2 uptake spans values from 1 to 4 GtC yr^{-1} (see Figure 11), less precise than the composite ^{13}C estimate of $2.10 \pm 0.93 \text{ GtC yr}^{-1}$ of HMR and the IPCC estimate of $2.0 \pm 0.8 \text{ GtC yr}^{-1}$, but in general agreement. The former result, $-0.025 \pm 0.002 \text{ ‰ yr}^{-1}$, suggests an oceanic uptake of CO_2 of $0.8 \pm 0.2 \text{ GtC yr}^{-1}$, less than the HMR and IPCC estimates. The indicated errors on our estimates represent only error due to uncertainty in the determination of the annual Suess effect at Bermuda, and do not include uncertainty in relating this effect to the uptake of CO_2 .

There are obvious uncertainties in the determination of the Suess effect in surface ocean water, mainly because of interannual variability. Extending the record at Bermuda would clearly help here, as would additional long-term measurements at other

locations where the interannual variability might be less. Measurements at other locations are also needed to check the spatial variability of the modeling results. Improving the three-dimensional modeling predictions of the surface water Suess effect are important, particularly in the region near Bermuda, where the spatial gradient of the Suess effect is large. Vertical monthly profiles of $\delta^{13}\text{C}$ through the thermocline at Bermuda should help elucidate the cause of the interannual variability.

The advantage to estimating the oceanic uptake of CO_2 from measurements of the surface ocean Suess effect relative to other methods employing ^{13}C is that adequate and representative data can probably be obtained with less effort. Of course, additional work must go into understanding the interannual variability, but other methods are not without similar problems. We have argued that if the box diffusion model is adjusted to predict the observed Suess effect in surface water, it should also predict the uptake of CO_2 . However, with measurements in major ocean regions, it may be possible to omit the box diffusion modeling step and directly constrain the three-dimensional model with the surface ocean Suess effect observations. The uptake of CO_2 by the oceans would then be determined directly from the three-dimensional model.

Acknowledgments. The authors thank Ernst Maier-Reimer and the Max-Planck-Institut für Meteorologie for making available their OGCM circulation field and for assistance in employing it. The manuscript has benefited from a careful review by Pieter Tans. The authors thank Yves Tourre for discussions of the Atlantic ENSO, and they appreciate critical comments by Ralph Keeling and Timothy Whorf. The authors have received support for this work from the National Aeronautics and Space Administration under grant NAGW-2987, the National Science Foundation under grant NSF ATM91-21986, and the Electric Power Research Institute.

References

- Bacastow, R. B., Modulation of atmospheric carbon dioxide by the Southern Oscillation, *Nature*, 261, 116-118, 1976.
- Bacastow, R. B., and C. D. Keeling, Pioneer effect correction to the observed airborne fraction, in *SCOPE 16: Carbon Cycle Modelling*, edited by B. Bolin, pp. 247-248, John Wiley, New York, 1981.
- Bacastow, R., and E. Maier-Reimer, Ocean-circulation model of the carbon cycle, *Clim. Dyn.*, 4, 95-125, 1990.
- Bacastow, R., and E. Maier-Reimer, Dissolved organic carbon in modeling oceanic new production, *Global Biogeochem. Cycles*, 5, 71-85, 1991.
- Broecker, W. S., and T. H. Peng, Evaluation of the ^{13}C constraint on the uptake of fossil fuel CO_2 by the ocean, *Global Biogeochem. Cycles*, 7, 619-626, 1993.
- Heimann, M., and E. Maier-Reimer, On the relations between the oceanic uptake of CO_2 and its carbon isotopes, *Rep. 149*, Max-Planck-Institut für Meteorologie, Hamburg, Germany, 1994.
- Houghton, J. T., L. G. Meira Filho, J. Bruce, Hoesung Lee, B. A. Callander, E. Haites, N. Harris, and K. Maskell (Eds.), *Climate Change 1994: Radiative Forcing of Climate Change and An Evaluation of the IPCC IS92 Emission Scenarios*, 339 pp., Cambridge University Press, New York, 1995.
- Keeling, C. D., The Suess Effect: ^{13}C Carbon- ^{14}C Carbon Interactions, *Environment International*, 2, 229-300, Pergamon, Tarrytown, N.J., 1979.
- Keeling, C. D., R. B. Bacastow, A. F. Carter, S. C. Piper, T. P. Whorf, M. Heimann, W. G. Mook, and H. Roeloffzen, A three-dimensional model of atmospheric CO_2 transport based on observed winds, 1, Analysis of observational data, in *Aspects of Climate Variability in the Pacific and Western Americas*, edited by D. H. Peterson, *Geophys. Monogr. Ser.*, vol 55, pp. 165-236, AGU, Washington, D.C., 1989.

- Jasper, J. P., and J. M. Hayes, A carbon isotope record of CO_2 levels during the late Quaternary, *Nature*, **34**, 462-464, 1990.
- Jones, P. D., S. C. B. Raper, R. S. Bradley, H. F. Diaz, P. M. Kelly, and T. M. L. Wigley, Northern Hemisphere surface air temperature variations: 1851-1984, *J. Clim. Appl. Meteorol.*, **25**, 161-179, 1986a.
- Jones, P. D., S. C. B. Raper, and T. M. L. Wigley, Southern Hemisphere surface air temperature variations, 1851-1984, *J. Clim. Appl. Meteorol.*, **25**, 1213-1230, 1986b.
- Maier-Reimer, E., Geochemical cycles in an ocean general circulation model: Preindustrial tracer distributions, *Global Biogeochem. Cycles*, **7**, 645-677, 1993.
- Maier-Reimer, E., and K. Hasselmann, Transport and storage of CO_2 in the ocean - An inorganic ocean-circulation carbon cycle model, *Clim. Dyn.*, **2**, 63-90, 1987.
- Maier-Reimer, E., U. Mikolajewicz, and K. Hasselmann, Mean circulation of the Hamburg LSG OGCM and its sensitivity to the thermohaline surface forcing, *J. Phys. Oceanogr.*, **23**, 731-757, 1993.
- Michaels, A. F., et al., Seasonal patterns of ocean biogeochemistry at the U.S. JGOFS Bermuda Atlantic Time-series Study site, *Deep Sea Res. Part 1*, **41**, 1013-1038, 1994.
- Menzel, D. W., and J. H. Ryther, The annual cycle of primary production in the Sargasso Sea off Bermuda, *Deep Sea Res.*, **35**, 351-366, 1960.
- Mook, W. G., J. C. Bommerson, and W. H. Staverman, Carbon isotope fractionation between dissolved bicarbonate and gaseous carbon dioxide, *Earth Planet. Sci. Lett.*, **22**, 169-176, 1974.
- Mook, W. G., M. Koopmans, A. F. Carter, and C. D. Keeling, Seasonal, latitudinal, and secular variation in the abundance and isotopic ratios of atmospheric carbon dioxide, 1. Results from land stations, *J. Geophys. Res.*, **88**, 10,915-10,933, 1983.
- Oeschger, H., U. Siegenthaler, U. Schotterer, and A. Gugelmann, A box diffusion model to study the carbon dioxide exchange in nature, *Tellus*, **27**, 168-192, 1975.
- Quay, P. D., B. Tilbrook, and C. S. Wong, Oceanic uptake of fossil fuel CO_2 : Carbon-13 evidence, *Science*, **256**, 74-79, 1992.
- Rau, G. H., T. Takahashi, D. J. Des Marais, Latitudinal variations in plankton $\delta^{13}\text{C}$: Implications for CO_2 and productivity in past oceans, *Nature*, **341**, 516-518, 1989.
- Reinsch, C. H., Smoothing by spline functions, *Numerische Mathematik*, **10**, 177-183, 1967.
- Revelle, R., and H. E. Suess, Carbon dioxide exchange between atmosphere and ocean, and the question of an increase of atmospheric CO_2 during the past decades, *Tellus*, **9**, 18-27, 1957.
- Siegel, D. A., A. F. Michaels, J. C. Sorensen, M. C. O'Brien, and M. A. Hammer, Seasonal variability of light availability and utilization in the Sargasso Sea, *J. Geophys. Res.*, **100**, 8695-8713, 1995.
- Siegenthaler, U., M. Heimann, and H. Oeschger, Model responses of the atmospheric CO_2 level and $^{13}\text{C}/^{12}\text{C}$ ratio to biogenic CO_2 input, in *Carbon Dioxide, Climate and Society*, edited by Jill Williams, pp. 79-87, Pergamon, Tarrytown, N.J., 1978.
- Siegenthaler, U., Uptake of excess CO_2 by an outcrop-diffusion model of the ocean, *J. Geophys. Res.*, **88**, 3599-3608, 1983.
- Tans, P. P., J. A. Berry, and R. F. Keeling, Oceanic $^{13}\text{C}/^{12}\text{C}$ Observations: A new window on ocean CO_2 uptake, *Global Biogeochem. Cycles*, **7**, 353-368, 1993.
- Tourre, Y. M., and W. B. White, ENSO signals in global upper-ocean temperature, *J. Phys. Oceanogr.*, **25**, 1317-1332, 1995.

R. B. Bacastow, C. D. Keeling, T. J. Lueker, and M. Wahlen, Scripps Institution of Oceanography, University of California, La Jolla, CA 92093-0220. (e-mail: rbacastow@ucsd.edu; cdkeeling@ucsd.edu; tlueker@ucsd.edu; mwahlen@ucsd.edu)

W. G. Mook, Isotope Physics Laboratory, University of Groningen, Nijenborgh 4, 9747 AG Groningen, Netherlands.

(Received August 17, 1995; revised January 17, 1996; accepted January 19, 1996.)